Grain refinement in 7475 aluminium alloy via high-pressure torsion and hydrostatic extrusion

K. Wawer[1]*, M. Lewandowska[1], A. Wieczorek[2,3], E. C. Aifantis[3], M. Zehetbauer[2], K. J. Kurzydlowski[1]

[1] *Warsaw University of Technology, Faculty of Materials Science and Engineering, Woloska 141, 02-507 Warsaw, Poland*
[2] *University of Vienna, Institute of Materials Physics, Boltzmanngasse 5, A-1090 Vienna, Austria*
[3] *Laboratory of Mechanics and Materials Politechnic School, Aristotle University of Thessaloniki, Greece*

Received 28 August 2008, received in revised form 14 May 2009, accepted 14 May 2009

Abstract

The aim of this work was to investigate the dependence of the microstructure and mechanical properties of 7475 aluminium alloy on the processing route via severe plastic deformation (SPD). To this end two SPD techniques were used: hydrostatic extrusion (HE) and high-pressure torsion (HPT). They were carried out at room temperature to approximately the same accumulated true strain. Prior processing, the samples were subjected to two different treatments: (i) solution annealing followed by water quenching and (ii) solution annealing, quenching and ageing. It was found that, although in general, SPD leads to a similar significant increase of mechanical strength, the properties depend on the initial microstructure and processing route. In the case of HE, the samples deformed immediately after quenching exhibit higher mechanical strength whereas for HPT, aged samples possess higher strength. The results are discussed in terms of the influence of processing parameters and initial microstructure on microstructure evolution of 7475 aluminium alloy.

K e y w o r d s: aluminium alloys, severe plastic deformation (SPD), hydrostatic extrusion (HE), high-pressure torsion (HPT), microstructure, mechanical properties

1. Introduction

Nanostructured materials are of a great interest as they exhibit high mechanical strength combined with acceptable ductility, which make them perspective for a number of industrial applications. Such applications require, however, efficient methods for their fabrication. In the case of metals, a number of techniques are based on severe plastic deformation (SPD). It has been already shown that they are an efficient way for grain refinement down to nanometer scale [1]. The available SPD techniques, such as equal channel angular pressing (ECAP), high pressure torsion (HPT), cyclic extrusion compression (CEC), accumulative roll bonding (ARB) and hydrostatic extrusion (HE), differ in a number of processing parameters and the forms of products. The comparison of already well-established SPD techniques such as ECAP, ARB and multi-axial compression/forgings (MAC/F) was reported previously [2, 3]. However, HE, as relatively new in this context, has not been fully compared with the others. The objective of this study is to compare microstructure and mechanical properties of an aluminium alloy subjected to HE and HPT, as such comparison is a basis for benchmarking hydro extrusion as an SPD technique. It also gives better insight into the effect of processing route on the microstructure and properties of SPD metals.

In the HE, a sample surrounded with the pressure-transmitting medium is extruded through a hole in a die. The friction is very low because of the pressure induced hydrodynamic lubrication. Due to negligibly small friction, very high strain rates and high deformation homogeneity are achieved. Additionally, HE offers the potential for producing fully dense bulk materials in a variety of forms: rods, wires of complex cross-section and small tubes. These are features often unattainable by other SPD techniques [4, 5].

*Corresponding author: tel.: +48 22 234 8740; fax: +48 22 234 8750; e-mail address: kingac@inmat.pw.edu.pl

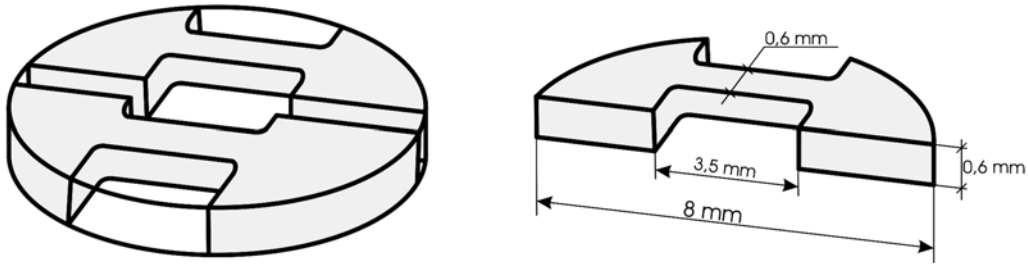

Fig. 1. Sample used in tensile test.

Table 1. Chemical composition of 7475 aluminium alloy (wt.%)

Alloy	Zn	Mg	Cu	Zr	Fe	Si	Ti	Mn
7475	6.00	2.49	1.66	0.12	0.12	0.094	0.015	0.01

In the HPT, a disc-like specimen is deformed by shear between two rotating anvils under compression force. The advantage of HPT method is the possibility to apply very high hydrostatic pressures. As a result, very large strains can be achieved at an expense of the volume of the processed materials [6, 7].

The microstructure evolution and the changes in mechanical properties during SPD processing depend not only on the deformation process but also on the initial microstructure of materials subjected to deformation [8]. For 2XXX aluminium alloy processed by HE, it was found, that precipitates strongly affect the process of grain refinement [9]. Combination of strengthening by grain refinement and phase transformation makes it possible to significantly improve the strength of precipitate strengthened alloys for high strength structural applications.

The aluminium alloys of 7xxx series are age--hardenable. They are subjected to solution annealing, water quenching and ageing to precipitate fine coherent particles, which improve strength of components of aircrafts and sporting goods [10, 11]. In the present study, heat treatment was combined with SPD processing in order to additionally improve mechanical strength via synergic effect of precipitates and grain size refinement.

2. Experimental

The material used in this study was an Al-Zn-Mg--Cu 7475 alloy. The chemical composition of the alloy is given in Table 1. The samples of this alloy were initially heat treated in two ways:

– solution annealed at 470 ℃ for 2 h and water quenched – samples designated as Q,

– solution annealed at 470 ℃ for 2 h, water quenched and aged at 160 ℃ for 24 h – samples designated as QA.

The samples (Q and QA) were processed at room temperature by HE and HPT to approximately the same accumulated true strain of ~ 3.8* and using a comparable hydrostatic pressure ($\sim$ 1 GPa). The HE deformation was performed in three consecutive steps: ø 20 → ø 10 → ø 5 → ø 3 mm. The extruded specimens were water cooled at the die exit. The samples for HPT had the form of discs with 8 mm in diameter and 0.8 mm in thickness. The discs were rotated by $\sim 81°$ to obtain approximately the same true strain at the parts of discs which were used for machining samples for mechanical testing and microstructure observations. The final true strain was calculated for radius 3 mm and was controlled during deformation by the time of rotation [12]. The processes of HE were carried out at the Institute of High Pressure Physics of the Polish Academy of Science whereas HPT at Erich Schmid Institute of Material Sciences at the Austrian Academy of Science.

The microstructures of the processed samples were examined by transmission electron microscopy. The foils were cut perpendicularly to the extrusion and compression direction for HE and HPT deformation, respectively. The DSC experiments were performed using a Netzsch DCS 204 calorimeter in a flowing Ar atmosphere with a constant heating rate of 10 K min^{-1} from 20 to 500 ℃. Three DSC runs without a reference sample were performed successively on each sample. Mechanical properties were determined by microtensile tests. The specimens for tensile tests, machined using spark erosion, had a cross section of 0.6 × 0.6 mm and a gauge length of 2.5 mm. Figure 1 shows the specimen shape and location within HPT disc. In the case of HE samples, the tensile specimens were cut parallel to extrusion direction. The tensile tests were performed at room temperature at a strain rate of 10^{-3} s^{-1}.

* The value of 3.8 is typical for HE and relatively low for HPT. It is employed for both processes for the sake of comparing results.

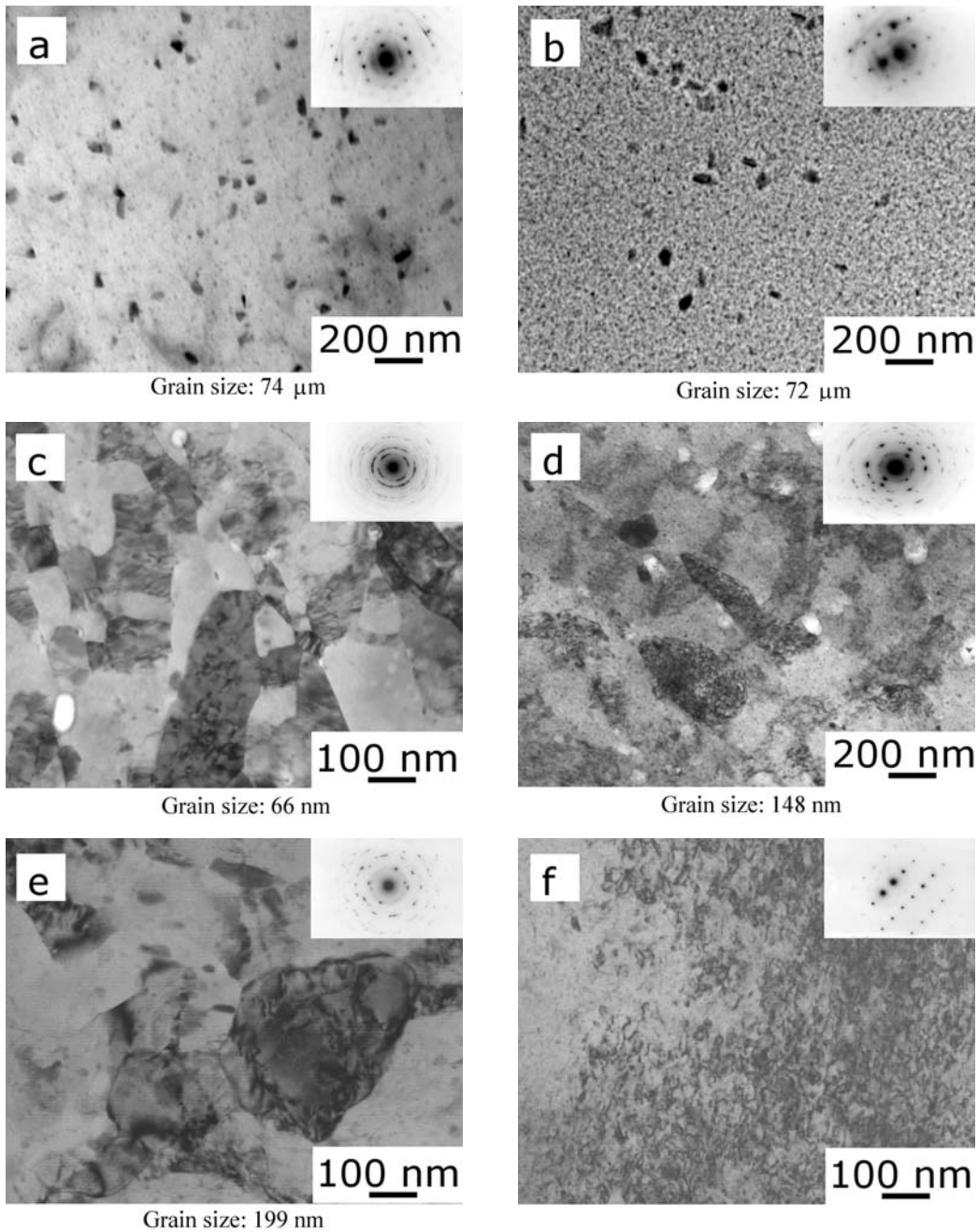

Fig. 2. TEM image of sample Q and QA before (a, b) and after HE (c, d) and HPT (e, f) deformation.

3. Results

3.1. TEM observations

TEM images of the microstructures of Q and QA samples, before and after deformation by HE and HPT, are presented in Fig. 2. Prior SPD, samples had coarse-grained microstructure with an average grain diameter of $\sim 70\,\mu m$. The microstructures contained also lamellar η phase precipitates with average size of $\sim 70\,nm$ (which were present in both Q and QA samples) and fine disc-shaped particles of metastable η' phase of the order $\sim 10\,nm$ (which were present in sample QA only). The volume fraction of η particles was comparable in both samples.

Both HE and HPT deformations bring about a significant grain refinement in the material processed immediately after quenching (Q samples). However, the measured average grain size is 66 nm in HE processed and 148 nm in HPT samples. Selected area electron diffraction (SAED) patterns (presented as inserts in TEM micrographs) taken from the area of the same diameter (7 μm) indicate larger misorientations between nanograins in the HE processed samples (dif-

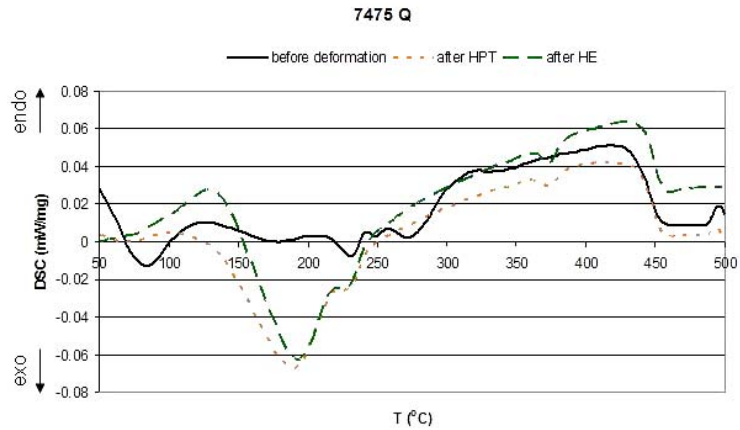

Fig. 3. DSC curves for 7475 Q sample before and after deformation.

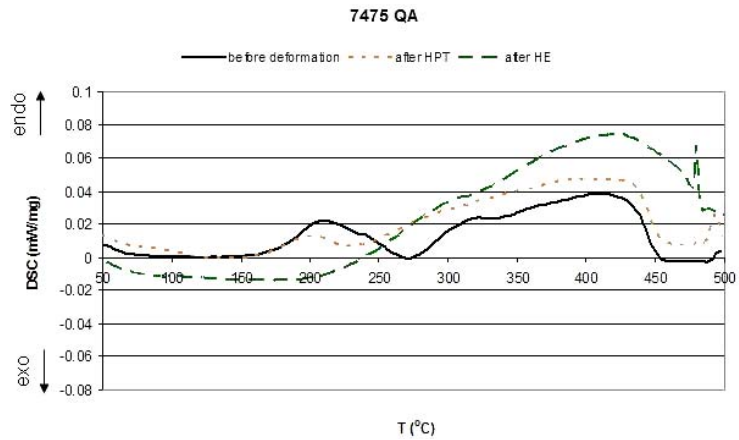

Fig. 4. DSC curves for 7475 QA sample before and after deformation.

fracted beams are spread into rings whereas in the case of HPT processed samples they are only slightly elongated).

In precipitation strengthened QA samples, HE processing leads to less developed and larger grains with the average grain size of 148 nm. In the HPT processed QA samples only a significant increase in the density of dislocations is observed. These dislocations are fairly homogenously distributed over the entire volume. SAED patterns of HE samples exhibit slightly spread diffraction spots (much less than in the case of Q samples). The HPT processed samples have diffraction pattern characteristic of a single crystal indicating no new grain formation.

3.2. DSC measurement

The comparison of DSC curves of 7475 aluminium alloys before and after HE/HPT deformation for samples Q and QA are presented in Figs. 3 and 4, respectively. Samples Q, before and after deformation, exhibit: (1) an endothermic peak at the temperature range of $\sim$ 70–150 ℃, (2) the exothermic effect including two overlapped peaks at the temperature range of $\sim$ 150–270 ℃, and (3) the endothermic effect at temperature range of $\sim$ 250–450 ℃. The literature data for 7xxx aluminium alloys [13–17] indicate that first endothermic peak is due to the dissolution of GP zones, the overlapping peaks at the temperature range of $\sim$ 150–270 ℃ correspond to the formation of phases η'/η and the second endothermic effect is due to the dissolution of η equilibrium phase.

It should be noted that SPD processing brings about a significant change in the curve shape when compared to the one for as-quenched material. After both HE and HPT deformation, the exothermic effect from the precipitation of η'/η occurs at a temperature 40 ℃ lower. The area of these exothermic peaks is larger for samples after deformation. This might be due to the high density of defects (dislocations and grain boundaries), which accelerate diffusion and thus the formation of η' and η precipitates in the material during deformation. On the other hand, only minor differences between DSC curves obtained for the materials processed either by HE or HPT are observed. The peak corresponding to GP zones dissolution is

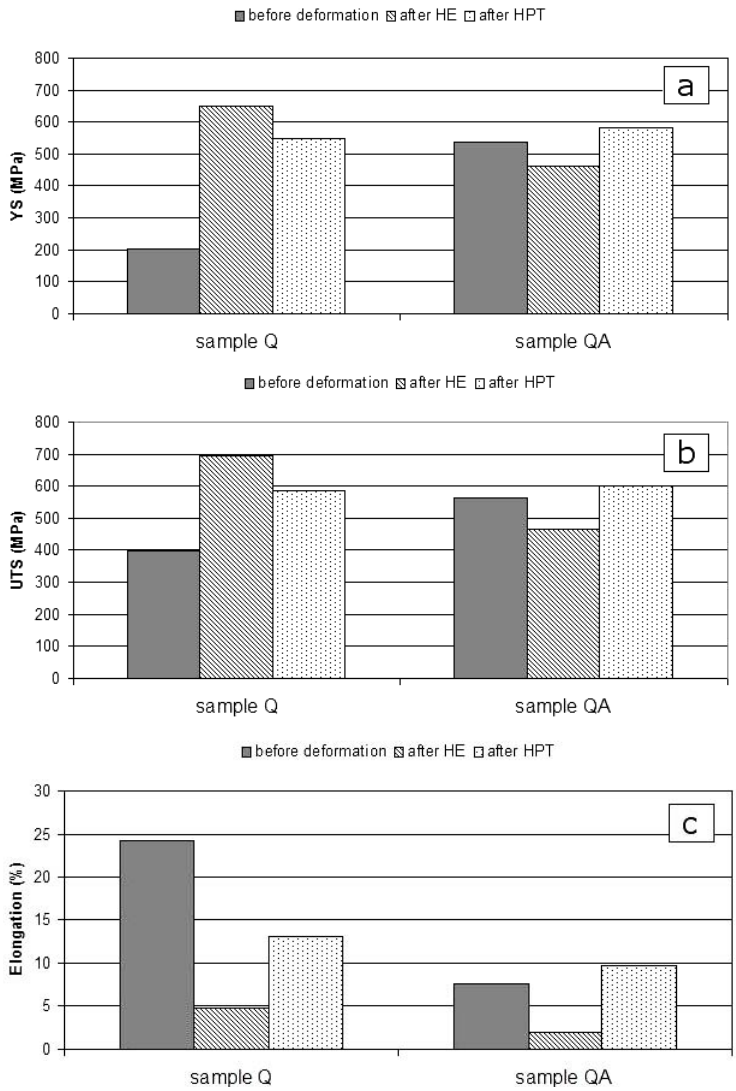

Fig. 5. Mechanical properties of 7475 after HE and HPT: (a) YS, (b) UTS, (c) elongation.

much smaller for the samples after HPT than HE deformation. It means that during HE processing (or shortly after that), GP zones precipitate in solution heat-treated matrix.

Samples QA reveal a microstructure containing mainly η' and η precipitates. As a result, in DSC curves one can distinguish two peaks: (1) first at the temperature range of $\sim$ 150–270 ℃ which corresponds to the dissolution of η' precipitates and (2) second in the temperature range $\sim$ 270–450 ℃ which is related to the dissolution of the equilibrium phase η. HPT deformation leads to a partial dissolution of η' (the peak characteristic for η' dissolution is smaller than in material without deformation). After HE deformation, the peaks corresponding to the dissolution of η' precipitates were not observed. This suggests that during HE or soon after the processing η' precipitates undergo dissolution.

3.3. Mechanical properties

The values of the yield stress, ultimate tensile strength (YS and UTS, respectively) and elongation of Q and QA samples after HE and HPT deformation are presented in Fig. 5. In the case of samples processed immediately after quenching, the two processing methods bring about a significant increase in mechanical strength. The YS increases from 205 MPa before deformation to 650 and 551 MPa after HE and HPT, respectively. It should be noted that the samples processed by HE exhibit higher yield and ultimate tensile strength. On the other hand, samples processed by HPT exhibit higher elongation to fracture.

In the case of QA samples, the strength is higher after HPT deformation. It should be noted that aged samples processed by HPT have higher elongation than before deformation whereas HE brings about plasticity reduction.

Table 2. The calculated temperature rise for the samples Q and QA during deformation by HE

Sample	Temperature rise ΔT (K)		
	ø20 → ø10 mm	ø10 → ø5 mm	ø5 → ø3 mm
7475 Q	281	337	245
7475 QA	380	403	216

4. Discussion

4.1. Effect of processing parameters on microstructure evolution

The microstructures of 7475 alloy processed by HE and HPT differ significantly in terms of grain size, grain boundary character and precipitates although they were obtained by applying the same true strain and pressure. However, these differences can be explained in terms of the influence of other processing parameters, in particular strain rate and temperature. The two deformation methods differ in strain rate, which in the case of HPT is $\sim 2 \times 10^{-2}\,\mathrm{s}^{-1}$ whereas for HE achieves the value of $\sim 1 \times 10^{2}\,\mathrm{s}^{-1}$. As a result, the time of the processing by HPT amounts to a few minutes whereas HE lasts only few seconds. Obviously, for low strain rate HPT process, the deformation proceeds at isothermal condition. The heat is dissipated into the surrounding with no major change in the temperature of the processed material. For high strain rate HE process, the conditions become close to adiabatic. In the adiabatic conditions, the energy of plastic deformation is transformed into heat and leads to a temperature rise. This temperature rise can be calculated from the following equation:

$$Q_{\mathrm{v}} = c\rho\Delta T, \tag{1}$$

where Q_{v} is value of heat per volume unit (Q_{v} is equal to the value of extrusion pressure which is registered during processing), c is specific heat ($9000\,\mathrm{J\,kg^{-1}\,K^{-1}}$ for pure aluminium), ρ is density ($2700\,\mathrm{kg\,m^{-3}}$ average density for 7475 aluminium alloy), ΔT is temperature rise.

The calculated temperature rise for individual extrusion steps for the samples studied in this work is given in Table 2. It varies from 245 to 337 ℃ for sample Q and from 216 to 403 ℃ for sample QA. The calculations were performed assuming that 90 % of plastic deformation work is converted into heat and the remaining part into stored energy. It should be noted that such relatively large temperature rise lasts only few seconds (as the HE process lasts only few seconds). However, it may induce significant changes in microstructure of the processed material. In the case of HPT deformation, one can assume that the process occurs at a constant room temperature.

The impulse-like temperature rise during HE accelerates diffusion and brings about precipitation in the metastable structures of Q and QA samples. In the case of quenched samples, it causes precipitation of GP zones. In the QA samples, transformation of $\eta' \rightarrow \eta$ takes place. Both processes are indirectly evidenced in DSC measurements. The heat generated during HE may also influence the processes of defects rearrangement and new grains formation. As a result, for the same true strain the grains are smaller and better developed in the case of HE processed samples.

Since HPT is assumed to proceed at a constant temperature, microstructure evolution is expected to result primarily from intensive shear deformation taking place during processing. The results indicate that a partial deformation induced dissolution of η' precipitates may occur, as supported by the results of DSC studies.

4.2. Effect of precipitates on grain refinement

The results have shown that Q and QA samples differ significantly in terms of the grain size refinement. The process of grain refinement is much more efficient in Q than QA billet. This indicates that precipitates have a detrimental effect on the process of grain refinement. Such their effect is fully understandable in view of the interactions between moving dislocations and precipitates during plastic deformation. Coherent precipitates, such as η', are shearable by dislocation. At sufficiently high stress, this may lead to their fragmentation and even dissolution. However, as long as they are present in the microstructure, they inhibit rearrangement of dislocations and formation of new grains. As a result, as-quenched materials are more prone to grain refinement. The process of grain refinement becomes efficient after precipitates being dissoluted in the matrix, what is expected to happen for HPT processed sample after significantly larger true strain.

4.3. Strengthening mechanism

The 7475 aluminium alloy can be strengthened by at least 3 mechanisms: (1) precipitation, (2) grain refinement and (3) dislocation strengthening. As shown in TEM observations, SPD deformation of 7475 aluminium alloy leads to grain refinement and also to the increase in the dislocation density. This implies room for a significant improvement of strength of the material. On the other hand, the deformation resulting in grain refinement and increase in dislocation density

may also induce changes in the precipitates, as discussed in the previous section. The YS of investigated samples processed by HE and HPT may be expressed as:

$$\sigma = \sigma_{GB} + \sigma_D + \sigma_P, \quad (2)$$

where σ is yield strength, σ_{GB} is strengthening due to grain refinement, σ_D is dislocation strengthening, σ_P is precipitation strengthening.

Among samples processed in the present study, the highest strength was obtained for sample Q processed by HE. This sample exhibits the smallest grain size (66 nm), increased density of dislocations and is strengthened by precipitates (GP zones). The Q samples processed by HPT have larger grain size (148 nm), similar dislocation density and only reduced strengthening from the precipitates (since only small amount of GP zones are presented after processing by HPT).

In the case of aged samples, the contribution of grain boundary strengthening is very limited (because the grains are refined to a modest degree). The main strengthening mechanism results from the presence of dislocations and is combined with precipitation strengthening. However, there are some differences in precipitation strengthening in samples processed by HE and HPT. In the HPT sample, strong η' precipitates are still present in the microstructure whereas in HE sample, they transform into stable η phase. As a result, the strengthening from precipitates is much smaller in the latter sample and its YS is lower than in HPT sample.

The results discussed in the present study indicate that microstructure evolution in age-hardenable Al alloy during plastic deformation involves grain refinement and precipitates transformation. The combination of these two processes decides about final mechanical properties in question. It was shown that for relatively low true strain (below 4) HE seems to be more effective in grain size refinement. However, the resulting properties depend on several factors and in some cases HPT processing leads to better mechanical properties.

5. Conclusions

Based on the presented results the following conclusions can be drawn:

1. Both HE and HPT are effective methods for nanostructure formation in 7475 aluminium alloy. However, the nanostructure parameters strongly depend on the initial microstructure of the processed materials. In particular, the presence of precipitates significantly reduces the ability to grain refinement.

2. The mechanical properties of SPD processed 7475 alloys depend on both deformation route and the initial microstructure.

– SPD processing of as-quenched 7475 alloy improves the strength but the strength increase is higher in the case of HE processed materials.

– In the case of aged samples, HPT processing results in higher mechanical strength. Also HPT processed samples exhibit generally better plasticity than HE processed ones.

Acknowledgements

This work was supported by the Polish Ministry for Science and Higher Education (grant number 3T08A 06430) and the European Union (project: RTN-DEFINO HPRN-CT-2002-00198).

References

[1] VALIEV, R. Z.: Solid State Phenomena, *114*, 2006, p. 7.
[2] EDDAHBI, M.—DEL VALLE, J. A.—PEREZ-PRADO, M. T.—RUANO, O. M.: Mater. Sci. Eng. A, *410–411*, 2005, p. 308.
[3] CHERUKURI, B.—NEDKOVA, T. S.—SRINVASAN, R.: Mater. Sci. Eng. A, *410*, 2005, p. 394.
[4] LEWANDOWSKA, M.—GRABACZ, H.—PACHLA, W.—MAZUR, A.—KURZYDLOWSKI, K. J.: Solid State Phenom., *101–102*, 2005, p. 65.
[5] LEWANDOWSKA, M.—KURZYDLOWSKI, K. J.: Materials Characterization, *55*, 2005, p. 395.
[6] ZEHETBAUER, M.—STÜWE, H. P.—VORHAUER, A.—SCHAFLER, E.—KOHOUT, J.: Adv. Eng. Materials, *5*, 2004, p. 330.
[7] SAKAI, G.—HORITA, Z.—LANGDON, T. G.: Mater. Sci. Eng. A, *393*, 2005, p. 344.
[8] LEWANDOWSKA, M.: Journal of Microscopy, *224*, 2006, p. 34.
[9] LEWANDOWSKA, M.: Microstructure and properties of aluminium alloys processed by hydrostatic extrusion. Oral presentation at E-MRS Fall Meeting 2006, Symposium I Warsaw, Publishing House of The Warsaw University of Technology 2006.
[10] ZHAO, Y. H.—LIAO, X. Z.—JIN, Z.—VALIEV, R. Z.—ZHU, Y. T.: Acta Materialia, *52*, 2004, p. 4589.
[11] IMMARIGEON, J. P.—HOLT, R. T.—KOUL, A. K.—ZHAO, L.—WALLACE, W.—BEDDOES, J. C.: Materials Characterization, *35*, 1995, p. 41.
[12] ZEHETBAUER, M. J.—KOHOUT, J.—SCHAFLER, E.—SACHSLEHNER, F.—DUBRAVINA, A.: Journal of Alloys and Compounds, *378*, 2004, p. 329.
[13] ZHAO, Y. H.—LIAO, X. Z.—JIN, Z.—VALIEV, R. Z.—ZHU, Y. T.: Acta Materialia, *52*, 2004, p. 4589.
[14] IMMARIGEON, J.-P.—HOLT, R. T.—KOUL, A. K.—ZHAO, L.—WALLACE, W.—BEDDOES, J. C.: Materials Characterization, *35*, 1995, p. 41.
[15] GAO, N.—STARINK, M. J.—FURUKAWA, M.—HORITA, Z.—XU, CH.—LANGDON, T. G.: Materials Science Forum, *503–504*, 2006, p. 275.

[16] STARINK, M. J.—GAO, N.—FURUKAWA, M.—HORSTA, Z.—XU, CH.—LANGDON, T. G.: Advanced Materials Science, *7*, 2004, p. 1.

[17] LI, X.—STARINK, M. J.: Materials Science Forum, *331–337*, 2000, p. 1071.